



ORIGINAL ARTICLE

Antitumor activity of nanoemulsion based on essential oil of *Pinus koraiensis* pinecones in MGC-803 tumor-bearing nude mice

Yandong Zhang, Chao Xin, Culin Cheng, Zhenyu Wang *

Department of Food Science and Engineering, School of Chemistry and Chemical Engineering, Harbin Institute of Technology, Harbin 150090, China

Received 13 August 2020; accepted 27 September 2020
Available online 7 October 2020

KEYWORDS

Essential oils;
Nanoemulsion;
Anti-tumor activity;
HIPPO/YAP signal pathway

Abstract Essential oil is the natural extract rich in terpenoids, showing various physiological activities. Our previous studies have proved that essential oil of *Pinus koraiensis* pinecones (PEO) can inhibit the proliferation of MGC-803 cells and promote cell apoptosis *in vitro* via the HIPPO/YAP signaling pathway. In this study, we prepared the PEO nanoemulsion and studied its physicochemical properties and anti-tumor activity in MGC-803 tumor-bearing nude mice. The PEO nanoemulsion showed good stability, with an average particle size of 46.87 nm, a zeta potential of 34.4 mV, and a polydispersity index (PDI) of 0.121. The results of anti-tumor experiments showed that the PEO nanoemulsion can effectively inhibit the growth of tumor and promote the apoptosis. In addition, immunohistochemical results showed that the PEO nanoemulsion could inhibit the proliferation of MGC-803 cells by down-regulating the expression of YAP1/TEAD and its target proteins CTGF, AREG and GLI2 to regulate the HIPPO/YAP signaling pathway and its downstream signaling pathway. This study could provide the theoretical basis for the application of essential oils.

© 2020 The Author(s). Published by Elsevier B.V. on behalf of King Saud University. This is an open access article under the CC BY-NC-ND license (<http://creativecommons.org/licenses/by-nc-nd/4.0/>).

1. Introduction

Essential oils (EOs) were the secondary metabolite of aromatic plants, which had widely physiological activities and were used in agriculture (Yuan et al., 2019), food (Granata et al., 2018), medicine (El-Abid et al., 2019) and cosmetics (Martins et al., 2014) industries for many years. EOs are complex mixtures of many volatile components, which have strong hydrophobicity and instability, and some have strong bad odors (Liu et al., 2020; Chuesiang et al., 2019). These characteristics limit the application of EOs although many reports have confirmed that

* Corresponding author at: 92 Xidazhi Street, Nangang District, Harbin, China.

E-mail address: WZY925075@126.com (Z. Wang).

Peer review under responsibility of King Saud University.



Production and hosting by Elsevier

EOs have good antibacterial (Aleksic and Knezevic, 2019), antioxidant (de Souza et al., 2019), antitumor Zhang et al., 2018a and insecticidal (Czerniewicz et al., 2018) activities. In order to improve the problems encountered in the application of EOs, the preparation of EOs into nanoemulsions have achieved good results (Dávila-Rodríguez et al., 2019; Ribes et al., 2019; Pascual-Villalobos et al., 2017).

Nanoemulsion is a kind of transparent or semi-transparent colloidal dispersion system with isotropic, thermodynamic and dynamic stability, and the particle size is 10–100 nm (Sedaghat et al., 2019). Encapsulating EOs with nanoemulsions is very important to improve their long-term stability and bioavailability (Prakash et al., 2018). Nanoemulsions include water phase, oil phase, surfactant, and cosurfactant, and the preparation methods include low-energy and high-energy (Leão et al., 2019). Low-energy method is spontaneous and does not require the sophisticated equipment, so it is relatively low-cost and easy to operate (Leão et al., 2019). However, the high-energy mainly relies on ultrasonic generator, microfluidizer or high-pressure homogenizer, and different mechanical devices have different characteristics (Páez-Hernández et al., 2019). Compared with microfluidization and high-pressure homogenization, ultrasonication can obtain nanoemulsions with smaller droplet size, narrower particle size distribution, stronger stability, and smaller amount of surfactant (Pongsumpun et al., 2020; Prakash et al., 2019). Titrimetric phase conversion (low-energy) combined with ultrasonication (high-energy) to prepare nanoemulsion with oil-in-water (O/W) can reduce the use of surfactant and obtain stable essential oil nanoemulsion quickly and efficiently (Ranganathan & Mahalingam, 2019).

Pinus koraiensis is an ancient and precious forest tree species, widely distributed in northeast China, Russia, Japan, and Korea due to its strong cold resistance (Qu et al., 2019). *P. koraiensis* pine nuts are well known for their antioxidative (Chen et al. 2011), anti-aging and immune-boosting properties, and widely consumed worldwide (Yang et al., 2017). The following is the production of a large number of pinecones wastes. As a by-product of picking pine seeds, pinecones are often burned or discarded, which results in environmental pollution and waste of resources, and it is very harmful to environment-friendly development (Hou et al., 2019). In order to improve this situation, there are more and more reports about pinecones (Lee et al., 2018). Many reports confirmed that pinecones extracts have a variety of physiological activities, including antioxidation (Wang et al., 2019), anti-tumor (Yi et al., 2019), and anti-radiation (Yi et al., 2018). However, most of the reports focus on the polyphenols of pinecones, and the researches on EOs of pinecones are rare, although many organs of *Pinus* plants are rich in EOs (Mitić et al., 2018). Our previous studies had proved that the essential oil from *P. koraiensis* pinecones (PEO) had good anti-tumor activity *in vitro* (Zhang et al., 2019). The results showed that the main components of PEO were α -Pinene (40.91%), Limonene (24.82%), and β -Pinene (7.04%). And PEO could inhibit the proliferation and migration of MGC-803 cells by regulating the HIPPO/YAP signal pathway, and could arrest the cell cycle in G2/M phase and promote apoptosis. In order to evaluate the anti-tumor activity of PEO *in vivo*, we constructed a nude mouse model of MGC-803 tumor-bearing. However, the hydrophobicity, volatility and strong irritation of PEO were not conducive to the experiment. Therefore, we had prepared

a PEO-based nanoemulsion, hoping to improve the dispersion and stability of PEO, reduce its irritation and increase its bioavailability in the body. At present, the research on essential oil nanoemulsion mainly focused on *in vitro* experiments, and there were few *in vivo* studies. There was no report on the anti-tumor activity of *P. koraiensis* pinecones essential oil nanoemulsion *in vivo*. So this study is of great significance for the research and development of anti-tumor drugs and the comprehensive utilization of *P. koraiensis* resources.

2. Material and methods

2.1. Preparation of plant material and essential oil

The preparation of essential oil was consistent with our previous research (Zhang et al., 2019). The *P. koraiensis* pinecones were purchased from Yichun Hongxing District Forestry Bureau (Yichun, China) in October 2018. The air-dried pinecones were selected and crushed into powder with particle size less than 800 μm . The essential oil of *P. koraiensis* pinecones (PEO) was obtained by hydrodistillation. The PEO was stored in sealed brown bottles at $-20\text{ }^{\circ}\text{C}$.

2.2. Selection of surfactants and cosurfactants

The non-ionic surfactants Tween 80 (HLB 15.0) and Span 80 (HLB 4.5) were selected and mixed according to different HLB values, as shown in Table 1. PEO was added as oil phase into the evenly mixed surfactant, which was stirred for 10 min by a magnetic stirrer (MYP13-2S, Chijiu, Shanghai, China) at 1000 rpm, during which deionized water was added dropwise (oil phase: surfactant: water phase = 1:1:8). The coarse emulsion was centrifuged at $25\text{ }^{\circ}\text{C}$, 1000g, 20 min. The mixed surfactant with the smallest upper layer volume after centrifugation was selected as the final surfactant.

The most suitable cosurfactant was selected from the four common cosurfactants of anhydrous ethanol, 1,2-propanediol, glycerol, and n-butanol. Surfactant that selected in the above steps and cosurfactant were mixed in the proportion of 1:1, and then selected the cosurfactant with the smallest upper volume after centrifugation according to the above steps.

2.3. Construction of pseudo-ternary phase diagram and formulation of nanoemulsion

The water titration method was used to construct the pseudo-ternary phase diagram (Li et al., 2019). The selected surfactant and cosurfactant were mixed evenly according to the mass

Table 1 Mixed surfactant systems with different HLB.

Mixed HLB	Span-80 (%)	Tween-80 (%)
5	93.46	6.54
7	74.77	25.23
9	56.07	43.93
11	37.38	62.62
13	18.69	81.31
15	0	100

ratios (Km) of 3:1, 5:1, and 7:1 as the mixed surfactants (MS). The essential oil and mixed surfactant were mixed at the mass ratios of 1:9, 2:8, 3:7, 4:6, 5:5, 6:4, 7:3, 8:2, and 9:1 (PEO:MS). The mixtures were stirred with magnetic stirrer at 1000 rpm for 10 min, during which deionized water was added drop by drop until the system became clear from turbid, and the volume of deionized water was recorded. Using Origin 9.0 software to draw pseudo-ternary phase diagram, and the Km with the largest area was the best formula.

The research of Nilesh et al. was referred to prepare PEO nanoemulsion, and the parameters were slightly adjusted (Nirmal et al., 2018). According to the mass ratios of PEO were 5%, 7.5% and 10%, 9 points on the pseudo-ternary phase diagram were selected as the formula of nanoemulsion, and the coarse emulsions were prepared according to the steps in 2.2. The O/W type coarse emulsions were obtained by titration phase conversion. The coarse emulsions were further processed by the ultrasonic cell breaker (JY92-IIN, Xinzhi, Ningbo, China) with 650 W for 5 min (2 s ON and 5 s OFF). Finally, PEO nanoemulsions were prepared. The mean droplet size and polydispersity index (PDI) of nanoemulsions were measured by a dynamic light scattering instrument (Malvern Instrument, Worcestershire, UK), and the formula with the smallest particle size was selected.

2.4. Physicochemical properties

The zeta potential was determined by a Zetasizer Nano-ZS90 (Malvern Instruments, Worcestershire, UK); the pH value was determined by a pH meter (PHS-3E, Leici, Shanghai, China) at 25 °C; the refractive index was determined by an Abbe type refractometer (WYA-2W, Shanghai, China) at 25 °C.

2.5. Transmission electron microscopy (TEM) analysis

The prepared PEO nanoemulsion was dropped on a copper grid covered with a carbon film, dried naturally and then dyed with a 2% phosphotungstic acid solution. Finally, a transmission electron microscope (Tecnai 12, Philips company holland) was used to observe the particle morphology and take pictures.

2.6. Antitumor activity of nanoemulsion in vivo

2.6.1. Animal experiment design

Male BALB/c nude mice (each mouse was 24–28 days old and weighed 12–16 g) were selected as experimental model animals. All experimental mice purchased from Beijing Charles River Experimental Animal Technology Co., Ltd. (SCXK (Jing) 2016-0006, Beijing, China). The experiment was approved by the experimental animal welfare ethics committee of Harbin Institute of Technology (IACUC-2019017). Paclitaxel (PTX) was selected as a positive drug in animal experiment.

Sixty BALB/c nude mice were adaptively fed in a sterile environment for one week. Ten mice were randomly selected as the normal group, and each mouse was subcutaneously injected with 0.2 mL normal saline in the right hind limb. The remaining fifty mice were subcutaneously injected with 0.2 mL MGC-803 cells suspension (5×10^6 cells/mL) in the right hind limb. The tumor volumes were calculated every day after tumor growth. When the average tumor volumes

were 100–300 mm³, the fifty mice were randomly divided into five groups (ten mice in each group): model group (normal saline), PTX group (10 mg·kg⁻¹, twice a week), PEO nanoemulsion low-dose group (PEO-nano-L:50 mg·kg⁻¹·d⁻¹, according to the mass concentration of PEO), PEO nanoemulsion high-dose group (PEO-nano-H:100 mg·kg⁻¹·d⁻¹, according to the mass concentration of PEO), and free-PEO (100 mg·kg⁻¹·d⁻¹, free essential oil). Mice in the normal group and model group were given 0.2 mL of normal saline by intragastric administration every day, while those in the PEO nanoemulsion treatment groups were given 0.2 mL nanoemulsion by intragastric administration every day according to the experimental design. Mice in the PTX group were given 0.2 mL paclitaxel injection (TAXOL, Bristol-Myers Squibb Company, USA) intraperitoneally twice a week according to the designed dose.

Mice were treated with drugs for three weeks. During the experiment, the mice were weighed every 48 h, and the length and width of tumors were measured also. The tumor volume (V) and relative tumor volume (RTV) were calculated according to the following formula:

$$V = \frac{1}{2}ab^2 \quad (1)$$

Where V represents tumor volume, a represents tumor long diameter, and b represents tumor short diameter.

$$RTV = \frac{V_t}{V_0} \quad (2)$$

Where RTV represents the relative tumor volume, V_t represents the tumor volume at the initial administration, and V_0 represents the tumor volume at each measurement.

2.6.2. Relative tumor proliferation rate and organ index

After stopping the drugs treatment for 24 h, the mice were collected blood from the orbit, and then sacrificed by cervical dislocation. The tumor, liver, kidney, and spleen were measured accurately. The relative tumor proliferation rate and organ index of mice were calculated according to the following formula:

$$T/C(\%) = \frac{RTV_t}{RTV_c} \times 100\% \quad (3)$$

Where $T/C(\%)$ represents relative tumor proliferation rate, RTV_c represents the relative tumor volume in the model group after 21 days of treatment, and RTV_t represents the relative tumor volume in drug treated groups after 21 days of treatment.

$$OI = \frac{m_o(\text{mg})}{m_w(\text{g})} \quad (4)$$

Where OI represents organ index, m_o represents the mass of the organs, in mg, and m_w represents the weight of the mice before execution, in g.

2.6.3. HE staining of spleen

The spleen tissues of mice were cleaned with normal saline and fixed with 4% paraformaldehyde for 24 h at room temperature. The fixed spleen tissue was embedded in paraffin and cut into 5 μm thick sections. The spleen tissue was dewaxed in xylene for 8 min and repeated twice. Then soaked in anhydrous ethanol, 95% ethanol, 80% ethanol, and 70% ethanol for 5 min respectively, and finally soaked in distilled water for 2 min. The slices were dyed with hematoxylin for 10 min and rinsed with tap water for about 10 min to remove excess

dye solution, then washed with distilled water. Differentiated in hydrochloric acid ethanol differentiation solution for 3 s, then washed with tap water for 5 min. Return blue in Scott solution for 3 min, and washed with distilled water for 3 min, and repeated for 3 times. The slices were dyed with eosin for 10 min and washed with 70% ethanol for 1 min, then dehydrate with 80% ethanol for 1 min, 95% ethanol for 5 min, and anhydrous ethanol for 5 min. Xylene was used for transparency for 2 times, each time for 5 min. Finally, the slices were sealed with neutral resin and photographed under an optical microscope.

2.6.4. Apoptosis detection of tumor tissues by TUNEL staining

The tumor tissues were fixed in 4% paraformaldehyde solution for 24 h. The tumor tissues were embedded in paraffin and sectioned. Dewaxing with xylene for 5 min, followed by hydration with 100%, 95%, 80% and 75% ethanol for 5 min. The slices were immersed in 1% Triton X-100 solution for 3–5 min, and then immersed in 3% H₂O₂ sealing solution for 10 min. Each sample was added with 100 μ L Proteinase K working solution and reacted at 37 °C for 30 min. Added 100 μ L DNase I reaction solution to each sample, and treated at room temperature for 10–30 min. The samples were dried with absorbent paper, and 50 μ L TdT enzyme reaction solution was added to each sample for 60 min at 37 °C; then 50 μ L Streptavidin-HRP working solution was added to each sample for 30 min at 37 °C; finally, 50 μ L DAB working solution was added to each sample for 30 s–5 min at room temperature. After the completion of each step, PBS buffer was used for cleaning for 3 times, each time for 5 min. Finally, the slices were photographed with optical microscope.

2.6.5. Immunohistochemistry

The tumor tissues of mice were cleaned with normal saline and then embedded in paraffin and sliced. Paraffin slices were dewaxed with xylene for 8 min and repeated twice, and treated with the xylene and anhydrous ethanol (1:1, V: V) for 5 min, followed by anhydrous ethanol, 95% ethanol, 85% ethanol, and 75% ethanol for 5 min each time. After 3 times of PBS cleaning, the antigen was repaired with 0.01 mol/L sodium citrate buffer (100 °C, 20 min). After natural cooling to room temperature, washed it with PBS, and incubated it with 3% H₂O₂ solution at room temperature for 10 min, and sealed it with 1–2% goat serum for 30 min. After removal of the blocking solution, 50 μ L rabbit monoclonal antibody was added to each section, and overnight at 4 °C. Added polymer adjuvant 1, and incubated at 37 °C for 20 min; added secondary antibody (YAP1, TEAD2, CTGF, AREG, and GLI2 monoclonal antibody), and incubated at room temperature for 2 h. DAB solution was used to develop color for 30 s, and hematoxylin was used to dye after cleaning. After washing by water, differentiating by alcohol, dehydrating, transparentizing, and sealing, the photos were taken under the optical microscope. We used Image-Pro Plus 6.0 software to analyze the mean of integrated optical density (IOD) of the positive reaction, and use the mean of IOD to express the relative expression of protein.

2.6.6. Determination of the YAP1, TEAD2, CTGF, AREG, and GLI2 expression in serum

All operations were carried out according to the instructions of ELISA kit (Shanghai Gefan Biotechnology Co., Ltd., China).

Mouse blood were placed at room temperature to coagulate naturally. After centrifuging for 15 min at 1000g, supernatants were collected for detection. The standard solutions were tested together with the serum samples. 100 μ L of the solution to be tested was added to each micropore (the blank control group was added 100 μ L of distilled water), followed by 50 μ L of enzyme conjugate (except for the blank control group). After sealing, incubated in 37 °C incubator for 1 h. Washed 5 times with washing solution, then dried with absorbent papers. 50 μ L of Substrate A and 50 μ L of Substrate B were added to each micropore. After reaction in dark for 15 min at room temperature, added 50 μ L of Stop solution to each well, and measured the OD values of each well at 450 nm wavelength within 30 min. Used ELISA Calc v 0.1 software (logit-log mode) to process data.

2.7. Statistical analysis

All experiments were repeated three times, and the data were expressed as mean \pm standard deviation. All statistical analyses were performed using SPSS Statistics 17.0 software for one-way ANOVA. The criterion for statistically significant results were $p < 0.05$.

3. Results

3.1. Selection of surfactants and cosurfactants

HLB values have an important influence on the formulation design of nanoemulsions, which are usually used to select surfactants in the preparation of nanoemulsions (Li et al., 2018). According to the HLB values (5, 7, 9, 11, 13, and 15) designed in Table 1, Tween-80 and Span-80 were mixed for experiments. After centrifugation, the volumes of the upper liquid were 7.50, 3.20, 2.50, 1.50, 0.50, and 0.00 mL, respectively. Therefore, when the HLB value was 15, the emulsifying effect of surfactant was the best. So, Tween-80 was the suitable surfactant for PEO. Glycerol, 1,2-propanediol, anhydrous ethanol, and n-butanol were mixed with Tween-80 in the mass ratio of 1:1 for next experiments. The results showed that the volumes of the upper liquid after centrifugation were 0.50, 0.00, 0.50, and 0.75 mL, respectively, which indicated that 1,2-propanediol was the suitable cosurfactant. Therefore, Tween-80 and 1,2-propanediol were selected as the surfactant and cosurfactant.

3.2. Construction of pseudo-ternary phase diagram and formulation of nanoemulsion

According to Km values of 3:1, 5:1, and 7:1, the pseudo-ternary phase diagrams of PEO nanoemulsion (Fig. 1) were drawn. The results showed that when Km value was 5:1, the forming area of PEO nanoemulsion was the widest (Fig. 1b). Therefore, the mass ratio of Tween-80 and 1,2-propanediol was chosen to be 5:1. According to the mass ratio of essential oil was 5%, 7.5%, and 10%, 9 points were selected from Fig. 1b as the formula for preparing PEO nanoemulsions and the average particle size and PDI were determined (Table 2). The results showed that when the formulation of nanoemulsion was 10% PEO, 20% mixed surfactant and 70% water, the average particle size and PDI of the nanoemulsion were the smallest, which were

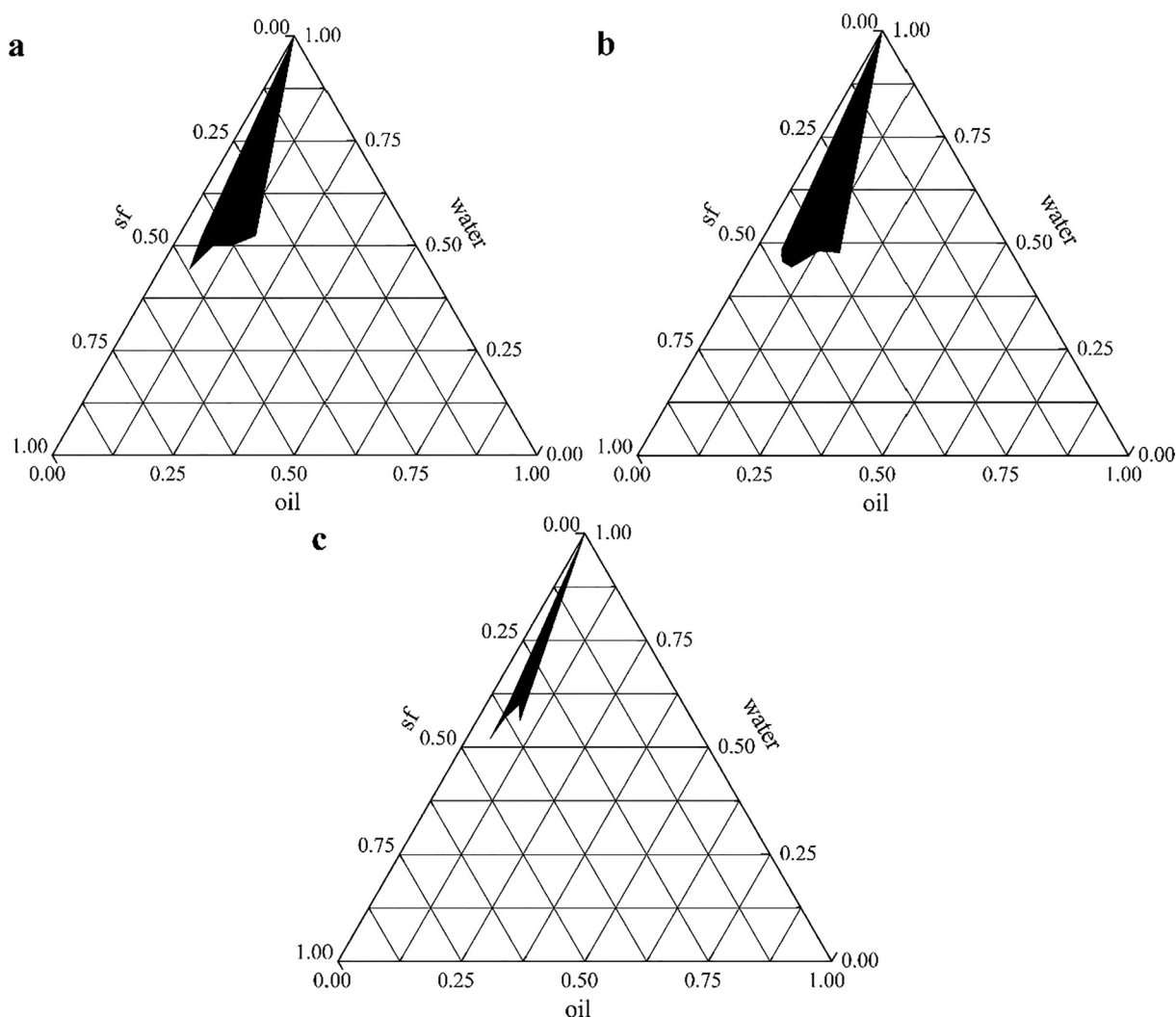


Fig. 1 The pseudo-ternary phase diagrams of PEO nanoemulsions (a: $K_m = 3:1$; b: $K_m = 5:1$; c: $K_m = 7:1$).

Table 2 Mixed surfactant systems with different HLB.

Number	PEO (%)	MS (%)	Deionized water (%)	Mean droplet size (nm)	PDI
1	5	10	85	237.30 ± 3.84	0.233 ± 0.017
2	5	15	80	61.42 ± 8.50	0.463 ± 0.074
3	5	20	75	153.70 ± 5.34	0.351 ± 0.036
4	7.5	15	77.5	204.05 ± 7.16	0.186 ± 0.068
5	7.5	20	72.5	190.60 ± 6.32	0.247 ± 0.011
6	7.5	25	67.5	167.20 ± 2.05	0.331 ± 0.026
7	10	20	70	46.87 ± 4.45	0.121 ± 0.026
8	10	25	65	314.00 ± 13.63	0.421 ± 0.021
9	10	30	60	240.31 ± 10.08	0.324 ± 0.047

46.87 nm and 0.121 respectively. Therefore, the final formula of PEO nanoemulsion is 10% essential oil, 20% mixed surfactant, and 70% deionized water.

3.3. Physicochemical characteristics of PEO nanoemulsion

The PEO nanoemulsion was prepared according to the formula determined in 3.2, as shown in Fig. 2. The nanoemulsion was clear, translucent and opalescent, and the Tyndall effect

appeared after irradiation with parallel light. Next, the physicochemical properties of the PEO nanoemulsion were studied. The zeta potential of this nanoemulsion were -34.4 ± 0.43 mV, indicating that the nanoemulsion was relatively stable. The refractive index of PEO nanoemulsion at 20 °C was 1.3742 ± 0.0011 , which was similar to the refractive index of pure water (1.3329 , 20 °C). This indicator showed that PEO nanoemulsion had good transparency. The nanoemulsion has a pH of 6.18 ± 0.01 at 20 °C, showing weak acidity.

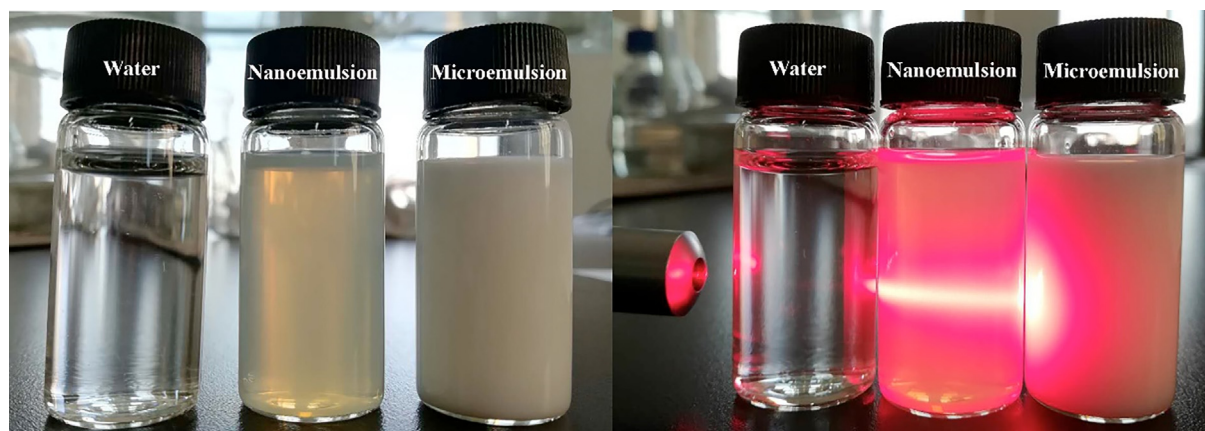


Fig. 2 The pictures of PEO nanoemulsions.

3.4. Morphological characteristics of PEO nanoemulsion

The morphological characteristics of PEO nanoemulsion were analyzed by transmission electron microscope (TEM), and the results were shown in Fig. 3. From the TEM image, it can be found that the particles were uniformly distributed in a spherical shape, with a particle size range of 30–70 nm. In addition, the particles in the PEO nanoemulsion were free to disperse without coagulation or agglomeration. These results were consistent with the particle size distribution and PDI measured by the dynamic light scattering instrument. Therefore, the finally obtained PEO nanoemulsion had a uniform spherical shape, a narrow particle size distribution range and can exist stably.

3.5. Anti-tumor activity and mechanism of PEO nanoemulsion in vivo

3.5.1. Effect of PEO nanoemulsion on tumor inhibition rate

Anti-tumor experiment in vivo showed that PEO nanoemulsion could inhibit the growth of tumors in MGC-803 tumor-bearing nude mice (Fig. 4). Fig. 4a showed the effect of PEO nanoemulsion on the body weights of mice. Through the changes of mice weight, it can be seen that the PEO nanoemulsion was

relatively mild for mice, and there was no big fluctuation of mice weight in each group on the whole. There was no death in the whole experiment. Fig. 4b was the tumor volume growth curve of tumor-bearing mice. It can be seen from the discount graph that the tumor volume of each group of mice was increasing, but from the slope of the broken line, it can be seen that the growth rate of the tumor was different, indicating that the effect of the drug on the tumor was different. Fig. 4c showed the relative tumor volumes of mice in each group after treatment. Compared with the model group, the relative tumor volumes of mice in the four treatment groups were decreased significantly ($p < 0.05$). There was no significant difference between the PEO-nano-L treatment group and the PTX treatment group or the free-PEO group ($p > 0.05$), while the relative tumor volume of the PEO-nano-H treatment group was significantly lower than that of the PTX treatment group and the free-PEO group ($p < 0.05$). This, along with the relative tumor proliferation rate (Fig. 4d), also proved the therapeutic effect of the drug on mice tumors. The relative tumor proliferation rate of mice in the PTX treatment group was 39.02%, the PEO-nano-L group was 36.95%, the PEO-nano-H group was 30.23%, and the free-PEO group was 34.57%. There were significant differences between the groups ($p < 0.05$). It is generally believed that anti-tumor drugs are effective when the relative tumor growth

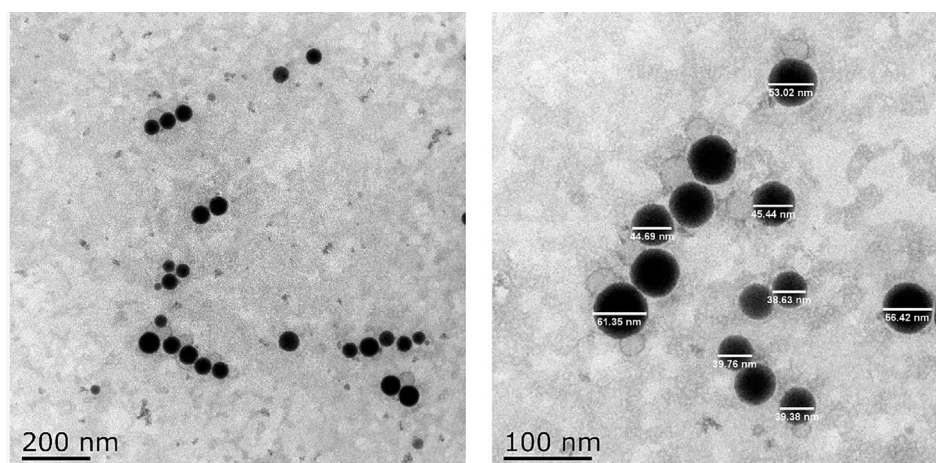


Fig. 3 Transmission electron microscope (TEM) images of PEO nanoemulsion at 200 nm scale bar and 100 nm scale bar.

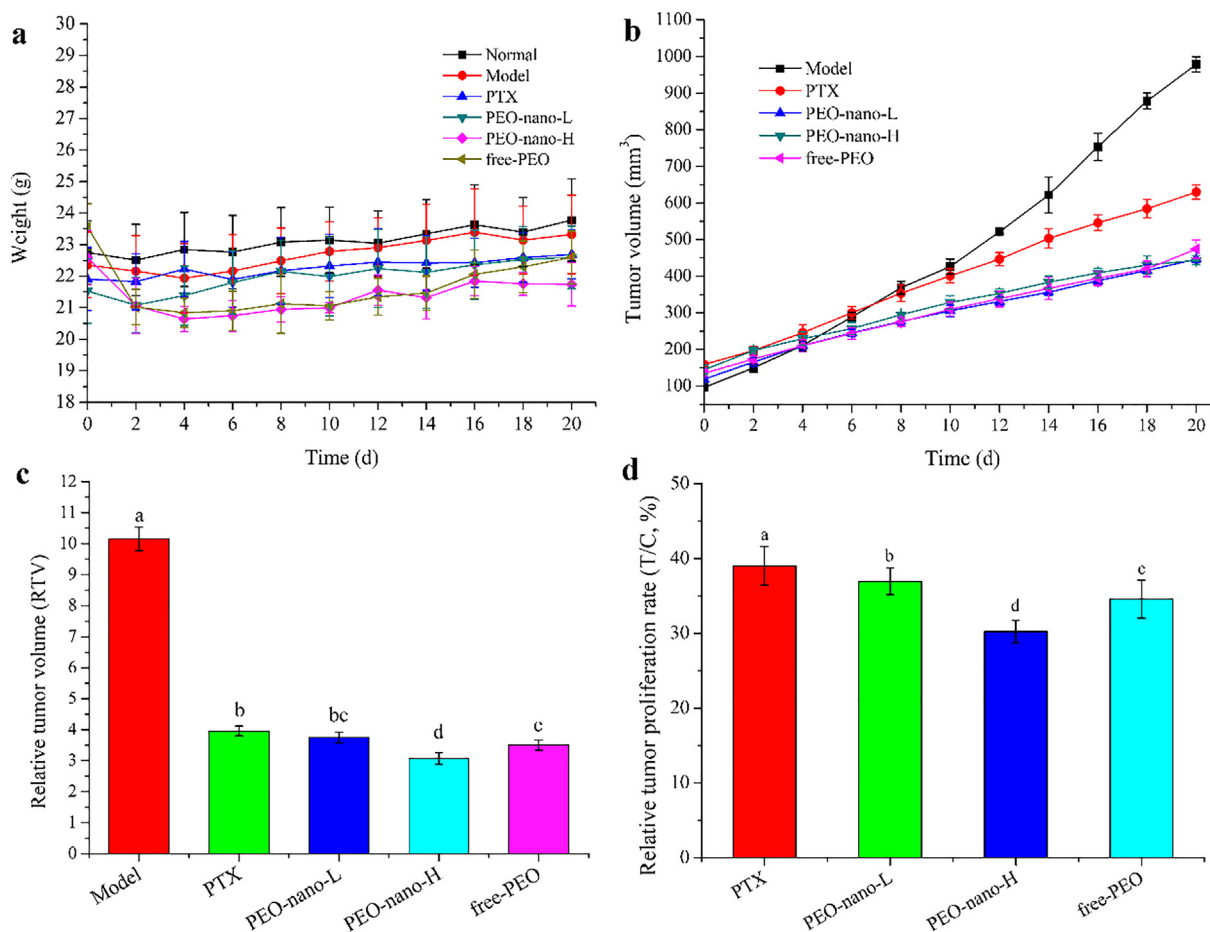


Fig. 4 The effect of PEO nanoemulsion on tumor inhibition rates of MGC-803 tumor-bearing nude mice. a represents the mouse body weight change curve; b represents the mouse tumor volume change curve; c represents the relative tumor volume of each group of mice; d represents the relative tumor proliferation rate of each group of mice ($n = 6$, different letters indicate significant differences, $p < 0.05$).

rate is less than 40%. Therefore, in this experiment, these four groups of drugs were effective in the treatment of MGC-803 tumor-bearing mice. And the high-dose group of PEO nanoemulsion had the best therapeutic effect.

3.5.2. Effect of PEO nanoemulsion on organ index and spleen HE staining

The organ index is a commonly used indicator of toxicology, which is simple and sensitive. This study calculated the liver index, kidney index and spleen index of mice (Fig. 5). The results showed that the liver index of mice in the positive control group was significantly higher than that in the normal group and model group (Fig. 5a, $**p < 0.01$, compared with normal group; $^{\#}p < 0.05$, compared with model group), which indicated that paclitaxel was toxic to the liver of mice in this experimental dose (10 mg/kg, intraperitoneal injection twice a week). However, there was no significant difference between the PEO nanoemulsion treatment groups and the normal group or the model group, and the same was true for the free-PEO treatment group ($p > 0.05$). These results indicated that PEO nanoemulsion and free PEO had no obvious toxicity to the liver of mice within the experimental dose range. Similarly, there were no significant changes in kidney index among the mice in each group (Fig. 5b, $p > 0.05$).

Different from liver index and kidney index, the spleen index of MGC-803 tumor-bearing mice were significantly increased compared with the normal group of mice (Fig. 5c, $**p < 0.01$, $***p < 0.001$). These results indicated that the inoculation of human gastric cancer cells caused excessive enlargement of the spleen of nude mice, which indicated that the spleen had entered the stage of negative immunoregulation from positive immunoregulation. This would promote tumor proliferation and metastasis, which was very detrimental to the survival of tumor-bearing mice. After drug treatment, the spleen index of mice in the PTX group was significantly higher than that of the model group, while the PEO nanoemulsion groups and the free-PEO group both improved. Among them, the PEO-nano-H group was significantly lower than the model group ($^{\#}p < 0.05$). These results indicated that a certain dose of PEO nanoemulsion can improve the hyperproliferation of the spleen of tumor-bearing mice and regulate the immunity of mice, which was of great significance for prolonging the life cycle of tumor-bearing mice.

The increase of the spleen index of tumor-bearing mice indicated that the proliferation of tumors had caused damage to the spleen of mice. HE staining was used to observe the changes of spleen tissue morphology of mice (Fig. 6). In the normal group, the morphology and structure of the spleen

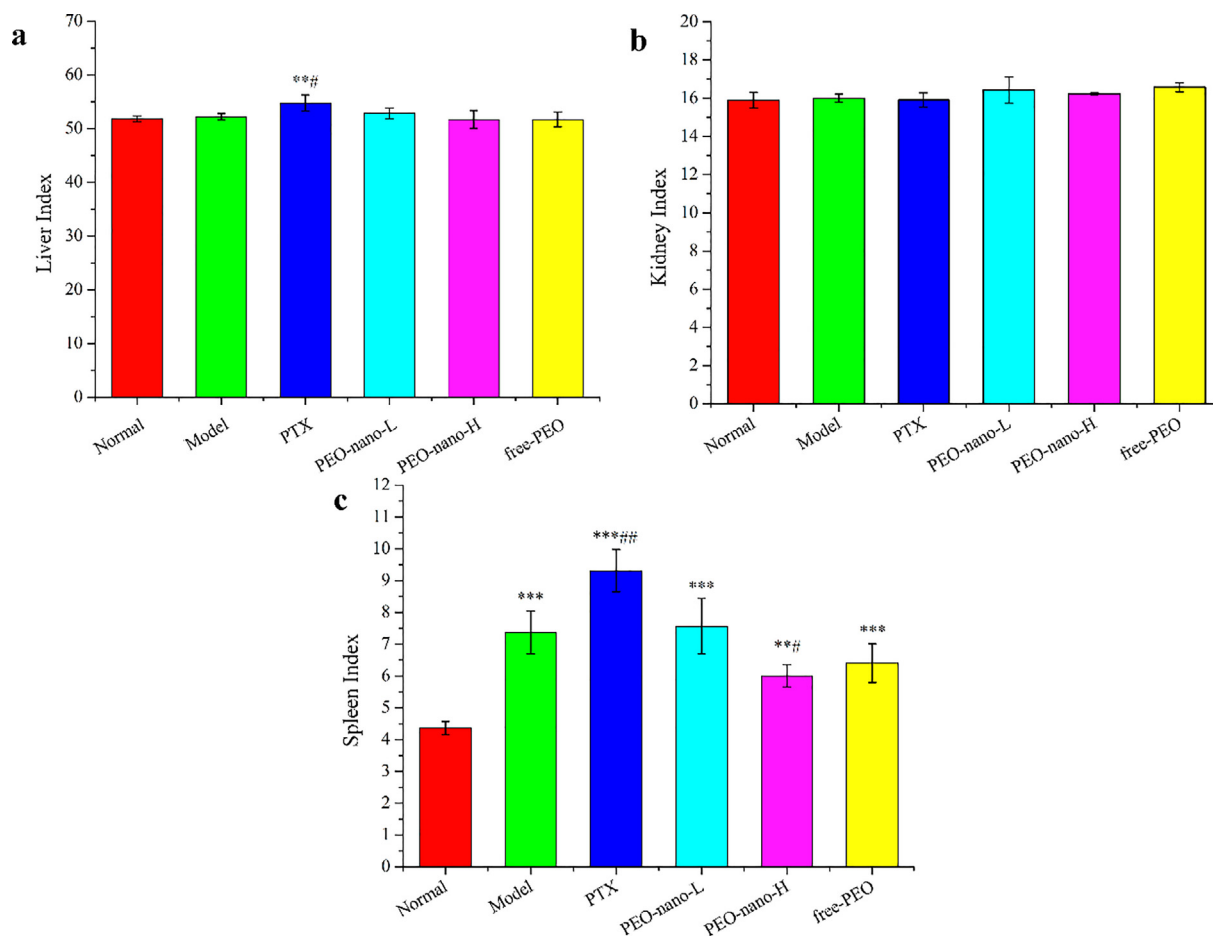


Fig. 5 The effect of PEO nanoemulsion on organ index of MGC-803 tumor-bearing nude mice. a-c represent liver index, kidney index, and spleen index, respectively ($n = 6$, $**p < 0.01$, $***p < 0.001$, compared with normal group; $\#p < 0.05$, $##p < 0.01$, $###p < 0.001$, compared with model group).

were normal with the white pulp, red pulp, and marginal area were clear, the distribution was uniform, the arrangement of lymphocytes were tight, and the structures of the spleen trabecula and corpuscle were complete (Fig. 6a). However, in the model group, the boundary between the white pulp and the red pulp was not clear, the distribution was disordered, the lymphocytes in the white pulp area were obviously reduced, and the immune ability of the body was decreased (Fig. 6b). The spleen tissue structure of the mice in the drugs treatment groups were improved that the boundary between the white pulp and the red pulp was gradually clear and the number of lymphocytes were gradually increased, and the effect of PEO nanoemulsion groups and free-PEO group were better than that of the PTX group (Fig. 6c-f). These results were consistent with the spleen index, demonstrating that PEO can alleviate spleen injury caused by the proliferation of tumors.

3.5.3. Effect of PEO nanoemulsion on tumor apoptosis

Apoptosis is a programmed death mode induced by physiological factors, which is the most common way for plant extracts to exert anti-tumor activity (Mirza et al., 2018; Zhang et al., 2018b). In this study, the TUNEL apoptosis detection kit was used to detect the apoptosis rates of tumor tissues in mice. As shown in Fig. 7. a-e, normal cells were purple and apoptotic cells were yellow-brown in the pictures. The results showed

that the apoptosis rates of the four drugs treatment groups were significantly higher than that of the model group (Fig. 7.f, $p < 0.05$), the apoptosis rates were 3.34% (model group), 28.00% (PTX group), 24.26% (PEO-nano-L group), 38.15% (PEO-nano-H group), and 22.94% (free-PEO group), respectively. The apoptosis rate of PEO-nano-H group was significantly higher than that of PEO-nano-L group and free-PEO group ($p < 0.05$), indicating that the therapeutic effect of PEO on tumor-bearing mice was related to the concentration and bioavailability of essential oil.

3.5.4. Effect of PEO nanoemulsion on immunohistochemistry

In this experiment, the expression levels of YAP1, TEAD2, CTGF, AREG and GLI2 proteins in the tumor tissues of MGC-803 tumor-bearing mice were detected by immunohistochemistry (Fig. 8). Fig. 8a was the photo of the tumor tissue sections of tumor-bearing mice after hematoxylin staining under the microscope. The larger the area and the darker the color of the yellow-brown parts in the pictures indicated the higher the proteins expression levels. YAP1, CTGF, AREG, and GLI2 were all over expressed in the tumor tissues of the model group (Fig. 8b-f), which were consistent with the reports. Compared with the model group, the expression levels of these four proteins were significantly down-regulated in the PEO nanoemulsion treatment groups and free-PEO treatment

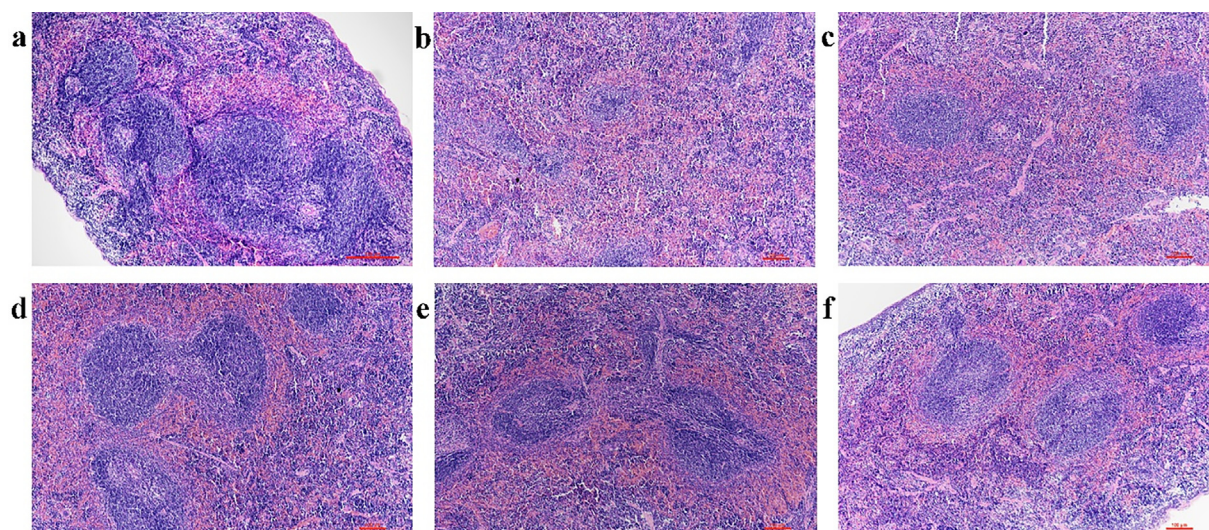


Fig. 6 The effect of PEO nanoemulsion on HE staining of spleen in MGC-803 tumor-bearing nude mice (magnification $\times 100$). a: Normal group; b: Model group; c: PTX group ($10 \text{ mg}\cdot\text{kg}^{-1}$, twice a week); d: PEO-nano-L ($50 \text{ mg}\cdot\text{kg}^{-1}\cdot\text{d}^{-1}$); e: PEO-nano-H ($100 \text{ mg}\cdot\text{kg}^{-1}\cdot\text{d}^{-1}$); f: free-PEO ($100 \text{ mg}\cdot\text{kg}^{-1}\cdot\text{d}^{-1}$).

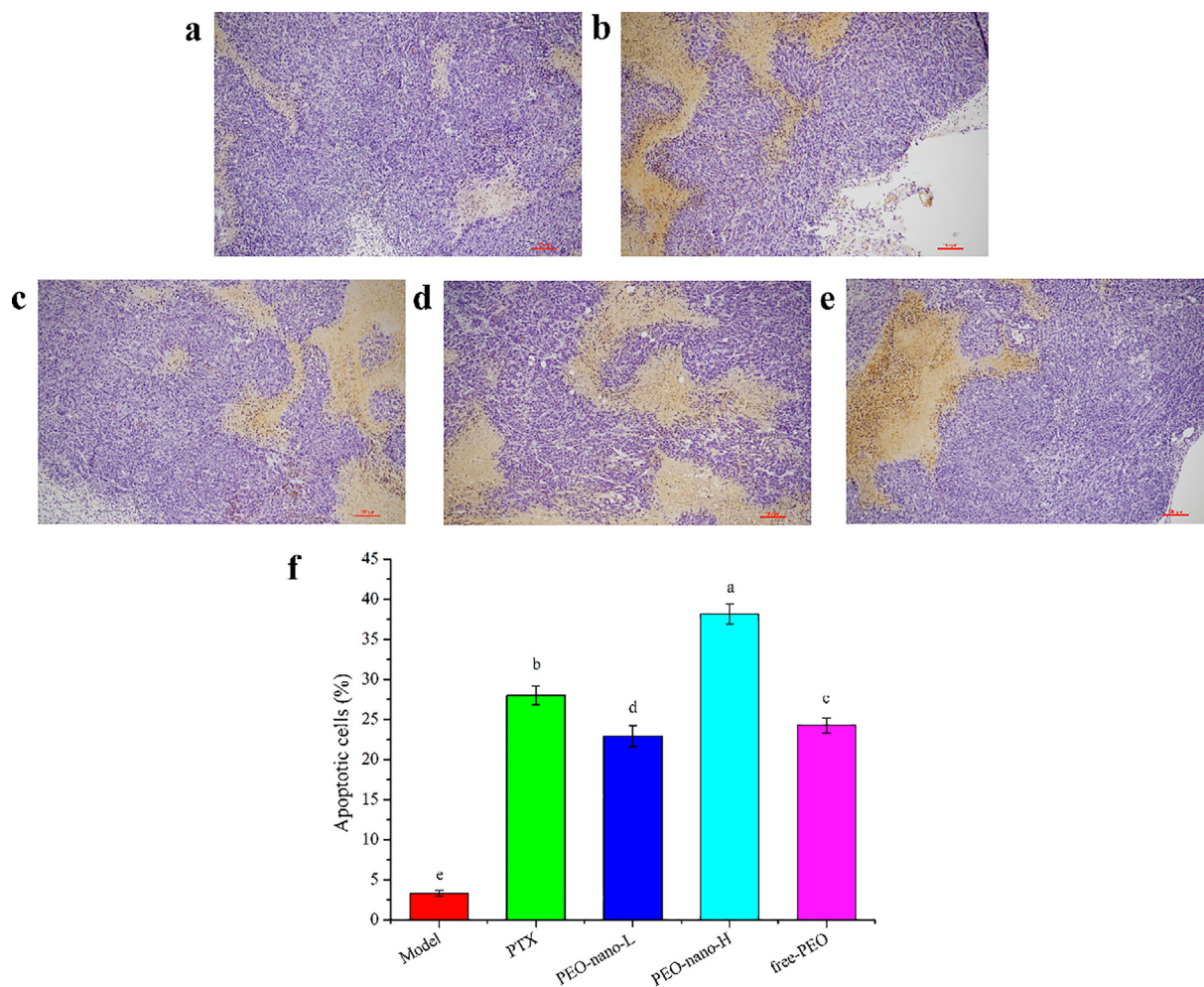


Fig. 7 The effect of PEO nanoemulsion on tumor apoptosis of MGC-803 tumor-bearing nude mice (magnification $\times 200$). a: Model group; b: PTX group ($10 \text{ mg}\cdot\text{kg}^{-1}$, twice a week); c: PEO-nano-L ($50 \text{ mg}\cdot\text{kg}^{-1}\cdot\text{d}^{-1}$); d: PEO-nano-H ($100 \text{ mg}\cdot\text{kg}^{-1}\cdot\text{d}^{-1}$); e: free-PEO ($100 \text{ mg}\cdot\text{kg}^{-1}\cdot\text{d}^{-1}$). f represents the apoptosis rate (apoptotic cell number/total cell number) in each group ($n = 6$, different letters indicate significant differences, $p < 0.05$).

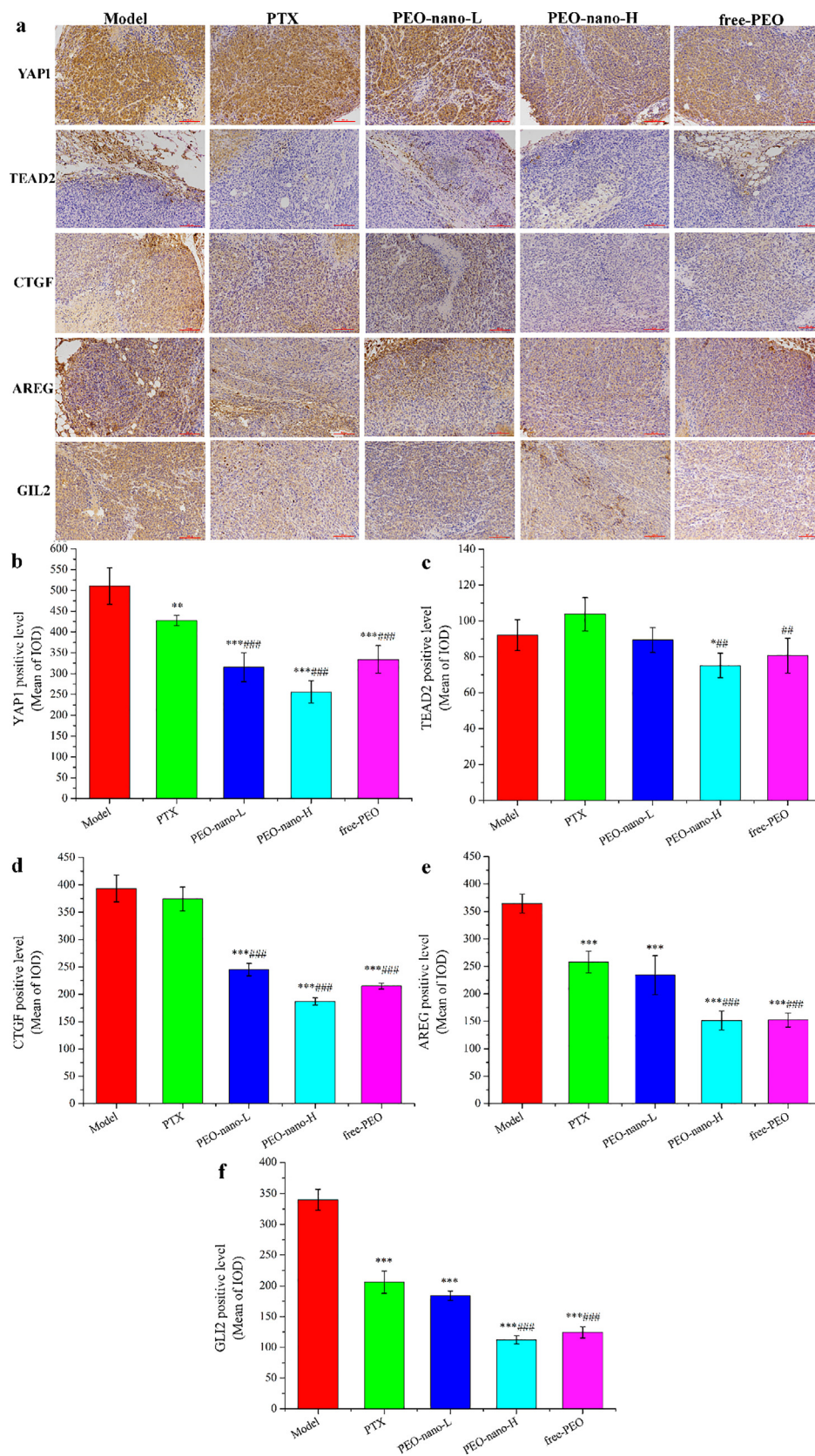


Fig. 8 The effect of PEO nanoemulsion on YAP1, TEAD2, CTGF, AREG, and GLI2 expression of tumor tissues in MGC-803 tumor-bearing nude mice. a: photos after hematoxylin staining (magnification $\times 200$); b-f: semi-quantitative analysis results ($n = 6$, $*p < 0.05$, $**p < 0.01$, $***p < 0.001$, compared with model group; $##p < 0.01$, $###p < 0.001$, compared with PTX-10 mg/kg group).

group (** $p < 0.001$). PTX can also significantly reduce the expression levels of the YAP1, AREG and GLI2 proteins (** $p < 0.01$, *** $p < 0.001$), but it had no significant effect on the CTGF protein ($p > 0.05$). Compared with YAP1, the expression levels of TEAD2 in tumor tissues were lower, and compared with the model group, only the PEO-nano-H group could significantly down-regulate the expression of TEAD2 (* $p < 0.05$). These results indicated that a certain concentration of PEO can reduce the expression levels of YAP1, TEAD2, CTGF, AREG and GLI2 proteins in the tumor tissues of MGC-803 tumor-bearing mice. The concentration of PEO in the PEO-nano-L group was insufficient, while the bioavailability of the free-PEO group was lower than that of the PEO-nano-H group, so these two groups had no significant effect on the expression level of TEAD2. At the same time, these results indicated that the anti-tumor mechanism of paclitaxel on MGC-803 cancer cells was different from that of *Pinus koraiensis* pinecones essential oil.

4. Discussion

Nanoemulsion can improve the water-insoluble properties, stability and bioavailability of EOs, which is of great significance for the application of EOs (Guerra-Rosas et al., 2017). Especially in the field of food and pharmaceutical industries, the improvements of hydrophobicity, stability and bad flavor for the EOs are particularly important, which have received more and more attention (Noori et al., 2018; Moraes-Lovison et al., 2017). In this study, the average particle size of the PEO nanoemulsion we prepared was 46.87 nm, and the average zeta potential was -34.4 mV, and TEM analysis found that it was a uniform spherical shape without agglomeration. These results all indicated that the PEO nanoemulsion was uniform and stable. This was a bold attempt for the application of PEO, which was beneficial to the application of EOs.

Observing the entire anti-tumor experiment, the high-dose group of PEO nanoemulsion showed better results in inhibiting tumor proliferation, promoting cell apoptosis and alleviating spleen damage in MGC-803 tumor-bearing mice. In the case of the same dosage form and administration method, the concentration of essential oil in the low-dose PEO nanoemulsion group was lower than that in the high-dose group, while the bioavailability of the free-PEO group was lower than that of the high-dose PEO nanoemulsion group at the same concentration of essential oil. Therefore, there were differences in the treatment effect between the three groups. These results indicated that the therapeutic effect of PEO on MGC-803 tumor-bearing mice was dose-dependent, and the nanoemulsion improved the bioavailability of PEO.

YAP1 is a core downstream effector of HIPPO signaling pathway, which is over expressed in many cancer types, including gastric cancer, and is recognized as a carcinogenic gene (Qiao et al., 2018; Maugeri-Saccà & De Maria, 2018). YAP1 does not have DNA binding domain and needs to play its transcriptional activity after binding with TEADs, but most reports believe that TEADs alone do not have the transcriptional activity (Lin et al., 2017). CTGF, AREG, and GLI2 are the downstream target genes of YAP1, and many reports have proved that CTGF, AREG, and GLI2 proteins are over expressed in many types of cancer tissues, including gastric cancer, which are the key for YAP1 to promote tumor cells

proliferation, migration, and tumor angiogenesis (Jiang et al., 2019; Wells et al., 2015; Xu et al., 2019). The results of our previous RNA sequencing showed that the TEAD2 was significantly down-regulated ($p < 0.05$) in MGC-803 cells after PEO treatment, while the other three subtypes (TEAD1, TEAD3, and TEAD4) in the TEAD family had no significant changes. Therefore, we detected the expression of YAP1/TEAD2 and their target proteins CTGF, AREG and GLI2 in tumor tissues of MGC-803 tumor-bearing mice by immunohistochemical techniques. The results showed that these proteins were over expressed in tumor tissues, and PEO nanoemulsion can significantly down-regulate the expression of these proteins ($p < 0.05$), thereby regulating the HIPPO/YAP signaling pathway and its downstream signaling pathways, which is consistent with the reports (Niu et al., 2019; Wang et al., 2017). These results indicated that PEO nanoemulsion can inhibit the proliferation of gastric cancer MGC-803 cells in mice by regulating the HIPPO/YAP signaling pathway and its downstream target pathways to achieve the purpose of tumor treatment.

5. Conclusion

In this experiment, the nanoemulsion prepared based on the essential oil of *P. koraiensis* pinecones had uniform particle size and good stability, which improved the water insolubility and volatility of the essential oil. The results of anti-tumor experiments proved that PEO nanoemulsion had a better therapeutic effect than free-PEO at the same concentration, which indirectly proved that nanoemulsion improved the bioavailability of PEO. Consistent with our previous anti-tumor activity experiments *in vitro*, the PEO nanoemulsion can down-regulate the expression of YAP1 protein and its target proteins CTGF, AREG and GLI2, and inhibit MGC-803 cells proliferation and promote apoptosis by regulating the HIPPO/YAP signaling pathway and its downstream signaling pathway. This study is of great significance for the application of essential oils and the comprehensive utilization of *P. koraiensis* resources, and it is also useful for the development of anti-tumor drugs for gastric cancer.

6. Ethics statement

The animal experiments part of this research complied with the guidelines for laboratory animal care and use, and had passed the Welfare Ethics Review of Experimental Animals by Harbin Institute of Technology. The Welfare Ethics Review Number is: IACUC-2019017.

Declaration of Competing Interest

The authors declare that they have no known competing financial interests or personal relationships that could have appeared to influence the work reported in this paper.

Acknowledgements

This research was funded by the Ministry of Science and Technology of the People's Republic of China, grant number 2016YFC0500305-02.

References

- Yuan, L., Yang, X., Yu, X., Wu, Y., Jiang, D., 2019. Resistance to insecticides and synergistic and antagonistic effects of essential oils on dimethfluthrin toxicity in a field population of *Culex quinquefasciatus* Say. *Ecotox. Environ. Safe.* 169, 928–936.
- Granata, G., Stracquadiano, S., Leonardi, M., Napoli, E., Consoli, G. M.L., Cafiso, V., Stefani, S., Geraci, C., 2018. Essential oils encapsulated in polymer-based nanocapsules as potential candidates for application in food preservation. *Food Chem.* 269, 286–292.
- El-Abid, H., Amaral, C., Cunha, S.C., Augusto, T.V., Fernandes, J.O., Correia-da-Silva, G., Teixeira, N., Moumni, M., 2019. Chemical composition and anti-cancer properties of *Juniperus oxycedrus* L. Essential oils on estrogen receptor-positive breast cancer cells. *J. Funct. Foods* 59, 261–271.
- Martins, I.M., Barreiro, M.F., Coelho, M., Rodrigues, A.E., 2014. Microencapsulation of essential oils with biodegradable polymeric carriers for cosmetic applications. *Chem. Eng. J.* 245, 191–200.
- Liu, Q., Zhang, M., Bhandari, B., Xu, J., Yang, C., 2020. Effects of nanoemulsion-based active coatings with composite mixture of star anise essential oil, polylysine, and nisin on the quality and shelf life of ready-to-eat Yao meat products. *Food Control* 107, 106771.
- Chuesiang, P., Siripatrawan, U., Sanguandekul, R., Yang, J.S., McClements, D.J., McLandsborough, L., 2019. Antimicrobial activity and chemical stability of cinnamon oil in oil-in-water nanoemulsions fabricated using the phase inversion temperature method. *LWT* 110, 190–196.
- Aleksic, S.V., Knezevic, P., 2019. Antimicrobial activity of *Eucalyptus camaldulensis* Dehn. Plant extracts and essential oils: A review. *Ind. Crop. Prod.* 132, 413–429.
- de Souza, W.F.M., Mariano, X.M., Isnard, J.L., de Souza, G.S., de Souza, G.A.L., de Carvalho, R.J.T., Rocha, C.B., Junior, C.L.S., Moreira, R.F.A., 2019. Evaluation of the volatile composition, toxicological and antioxidant potentials of the essential oils and teas of commercial Chilean boldo samples. *Food Res. Int.* 124, 27–33.
- Zhang, J., Huang, R., Cao, H., Cheng, A., Jiang, C., Liao, Z., Liu, C., Sun, J., 2018a. Chemical composition, in vitro anti-tumor activities and related mechanisms of the essential oil from the roots of *Potentilla discolor*. *Ind. Crop. Prod.* 113, 19–27.
- Czerniewicz, P., Chrzanowski, G., Sprawka, I., Sytykiewicz, H., 2018. Aphicidal activity of selected Asteraceae essential oils and their effect on enzyme activities of the green peach aphid, *Myzus persicae* (Sulzer). *Pestic. Biochem. Phys.* 145, 84–92.
- Dávila-Rodríguez, M., López-Malo, A., Palou, E., Ramírez-Corona, N., Jiménez-Munguía, M.T., 2019. Antimicrobial activity of nanoemulsions of cinnamon, rosemary, and oregano essential oils on fresh celery. *LWT* 112, 108247.
- Ribes, S., Fuentes, A., Barat, J.M., 2019. Effect of oregano (*Origanum vulgare* L. Ssp. *Hirtum*) and clove (*Eugenia* spp.) nanoemulsions on *Zygosaccharomyces bailii* survival in salad dressings. *Food Chem.* 295, 630–636.
- Pascual-Villalobos, M.J., Cantó-Tejero, M., Vallejo, R., Guirao, P., Rodríguez-Rojo, S., Cocero, M.J., 2017. Use of nanoemulsions of plant essential oils as aphid repellents. *Ind. Crop. Prod.* 110, 45–57.
- Sedaghat, D.A., Van Camp, J., Dewettinck, K., Van der Meeren, P., 2019. Production of thymol nanoemulsions stabilized using Quilaja Saponin as a biosurfactant: Antioxidant activity enhancement. *Food Chem.* 293, 134–143.
- Prakash, A., Baskaran, R., Paramasivam, N., Vadivel, V., 2018. Essential oil based nanoemulsions to improve the microbial quality of minimally processed fruits and vegetables: A review. *Food Res. Int.* 111, 509–523.
- Leão, K.M.M., Reis, L.V.C., Speranza, P., Rodrigues, A.P., Ribeiro, A.P.B., Macedo, J.A., Macedo, G.A., 2019. Physicochemical characterization and antimicrobial activity in novel systems containing buriti oil and structured lipids nanoemulsions. *Biotechnol. Rep.* 24, 365.
- Páez-Hernández, G., Mondragón-Cortez, P., Espinosa-Andrews, H., 2019. Developing curcumin nanoemulsions by high-intensity methods: Impact of ultrasonication and microfluidization parameters. *LWT* 111, 291–300.
- Pongsumpun, P., Iwamoto, S., Siripatrawan, U., 2020. Response surface methodology for optimization of cinnamon essential oil nanoemulsion with improved stability and antifungal activity. *Ultrason. Sonochem.* 60, 104604.
- Prakash, A., Vadivel, V., Rubini, D., Nithyanand, P., 2019. Antibacterial and antibiofilm activities of linalool nanoemulsions against *Salmonella Typhimurium*. *Food Biosci.* 28, 57–65.
- Ranganathan, N., Mahalingam, G., 2019. 2,4,6-Triphenylaniline nanoemulsion formulation, optimization, and its application in type 2 diabetes mellitus. *J. Cell. Physiol.* 234 (12), 22505–22516.
- Qu, H., Gao, X., Zhao, H., Wang, Z., Yi, J., 2019. Structural characterization and in vitro hepatoprotective activity of polysaccharide from pine nut (*Pinus koraiensis* Sieb. Et Zucc.). *Carbohydr. Polym.* 223, 115056.
- Chen, X., Zhang, Y., Wang, Z., Zu, Y., 2011. In vivo antioxidant activity of *Pinus koraiensis* nut oil obtained by optimised supercritical carbon dioxide extraction. *Nat. Prod. Res.* 25 (19), 1807–1816.
- Yang, R., Li, X., Lin, S., Zhang, Z., Chen, F., 2017. Identification of novel peptides from 3 to 10kDa pine nut (*Pinus koraiensis*) meal protein, with an exploration of the relationship between their antioxidant activities and secondary structure. *Food Chem.* 219, 311–320.
- Hou, K., Bao, M., Wang, L., Zhang, H., Yang, L., Zhao, H., Wang, Z., 2019. Aqueous enzymatic pretreatment ionic liquid–lithium salt-based microwave-assisted extraction of essential oil and procyanidins from pinecones of *Pinus koraiensis*. *J. Clean. Prod.* 236, 117581.
- Lee, T.K., Park, J.Y., Yu, J.S., Jang, T.S., Oh, S.T., Pang, C., Ko, Y., Kang, K.S., Kim, K.H., 2018. 7A,15-Dihydroxydehydroabietic acid from *Pinus koraiensis* inhibits the promotion of angiogenesis through downregulation of VEGF, p-Akt and p-ERK in HUVECs. *Bioorg. Med. Chem. Lett.* 28 (6), 1084–1089.
- Wang, L., Li, X., Wang, H., 2019. Physicochemical properties, bioaccessibility and antioxidant activity of the polyphenols from pine cones of *Pinus koraiensis*. *Int. J. Biol. Macromol.* 126, 385–391.
- Yi, J., Li, S., Wang, C., Cao, N., Qu, H., Cheng, C., Wang, Z., Wang, L., Zhou, L., 2019. Potential applications of polyphenols on main ncRNAs regulations as novel therapeutic strategy for cancer. *Biomed. Pharmacother.* 113, 108703.
- Yi, J., Cheng, C., Li, S., Wang, D., Wang, L., Wang, Z., 2018. Preparation optimization and protective effect on ⁶⁰Co-γ radiation damage of *Pinus koraiensis* pinecone polyphenols microspheres. *Int. J. Biol. Macromol.* 113, 583–591.
- Mitić, Z.S., Jovanović, B., Jovanović, S., Mihajilov-Krstev, T., Stojanović-Radić, Z.Z., Cvetković, V.J., Mitrović, T.L., Marin, P.D., Zlatković, B.K., Stojanović, G.S., 2018. Comparative study of the essential oils of four *Pinus* species: Chemical composition, antimicrobial and insect larvicidal activity. *Ind. Crop. Prod.* 111, 55–62.
- Zhang, Y., Xin, C., Qiu, J., Wang, Z., 2019. Essential Oil from *Pinus Koraiensis* Pinecones Inhibits Gastric Cancer Cells via the HIPPO/YAP Signaling Pathway. *Molecules* 24 (21), 3851.
- Li, T., Han, X., Bao, R., Hao, Y., Li, S., 2019. Preparation and properties of water-in-oil shiitake mushroom polysaccharide nanoemulsion. *Int. J. Biol. Macromol.* 140, 343–349.
- Nirmal, N.P., Mereddy, R., Li, L., Sultanbawa, Y., 2018. Formulation, characterisation and antibacterial activity of lemon myrtle and anise myrtle essential oil in water nanoemulsion. *Food Chem.* 254, 1–7.

- Li, Z., Cai, M., Liu, Y., Sun, P., 2018. Development of finger citron (*Citrus medica* L. Var. *Sarcodactylis*) essential oil loaded nanoemulsion and its antimicrobial activity. *Food Control* 94, 317–323.
- Mirza, M.B., Elkady, A.I., Al-Attar, A.M., Syed, F.Q., Mohammed, F.A., Hakeem, K.R., 2018. Induction of apoptosis and cell cycle arrest by ethyl acetate fraction of *Phoenix dactylifera* L. (Ajwa dates) in prostate cancer cells. *J. Ethnopharmacol.* 218, 35–44.
- Zhang, Y., Chen, S., Wei, C., Rankin, G.O., Ye, X., Chen, Y.C., 2018b. Flavonoids from Chinese bayberry leaves induced apoptosis and G1 cell cycle arrest via Erk pathway in ovarian cancer cells. *Eur. J. Med. Chem.* 147, 218–226.
- Guerra-Rosas, M.I., Morales-Castro, J., Cubero-Márquez, M.A., Salvia-Trujillo, L., Martín-Belloso, O., 2017. Antimicrobial activity of nanoemulsions containing essential oils and high methoxyl pectin during long-term storage. *Food Control* 77, 131–138.
- Noori, S., Zeynali, F., Almasi, H., 2018. Antimicrobial and antioxidant efficiency of nanoemulsion-based edible coating containing ginger (*Zingiber officinale*) essential oil and its effect on safety and quality attributes of chicken breast fillets. *Food Control* 84, 312–320.
- Moraes-Lovison, M., Marostegan, L.F.P., Peres, M.S., Menezes, I.F., Ghiraldi, M., Rodrigues, R.A.F., Fernandes, A.M., Pinho, S.C., 2017. Nanoemulsions encapsulating oregano essential oil: Production, stability, antibacterial activity and incorporation in chicken pâté. *LWT* 77, 233–240.
- Qiao, Y., Li, T., Zheng, S., Wang, H., 2018. The Hippo pathway as a drug target in gastric cancer. *Cancer Lett.* 420, 14–25.
- Maugeri-Saccà, M., De Maria, R., 2018. The Hippo pathway in normal development and cancer. *Pharmacol. Therapeut.* 186, 60–72.
- Lin, K.C., Park, H.W., Guan, K., 2017. Regulation of the hippo pathway transcription factor TEAD. *Trends Biochem. Sci.* 42 (11), 862–872.
- Jiang, J., Zhao, W., Tang, Q., Wang, B., Li, X., Feng, Z., 2019. Over expression of amphiregulin promoted malignant progression in gastric cancer. *Pathol. – Res. Pract.* 215, (10) 152576.
- Wells, J.E., Howlett, M., Cole, C.H., Kees, U.R., 2015. Deregulated expression of connective tissue growth factor (CTGF/CCN2) is linked to poor outcome in human cancer. *Int. J. Cancer* 137 (3), 504–511.
- Xu, S., Zhang, H., Chong, Y., Guan, B., Guo, P., 2019. YAP promotes VEGFA expression and tumor angiogenesis through gli2 in human renal cell carcinoma. *Arch. Med. Res.* 50 (4), 225–233.
- Niu, J., Ma, J., Guan, X., Zhao, X., Li, P., Zhang, M., 2019. Correlation between doppler ultrasound blood flow parameters and angiogenesis and proliferation activity in breast cancer. *Med. Sci. Monitor.* 25, 7035–7041.
- Wang, C., Huang, Y., Wang, S., Huang, Y., Tsai, C., Zhao, Y., Huang, B., Xu, G., Fong, Y., Tang, C., 2017. Amphiregulin enhances VEGF-A production in human chondrosarcoma cells and promotes angiogenesis by inhibiting miR-206 via FAK/c-Src/PKC δ pathway. *Cancer Lett.* 385, 261–270.